ISSN: 2096-3246
Volume 58, Issue 01, 2026

THE ROLE OF PR_2O_3 AND BARIUM OXIDE CONCENTRATION IN THE RADIATION PROTECTION EFFICIENCY OF SODIUM-LEAD BORATE GLASSES.

Susheela K Lenkennavar[1] and B. M. Praveen[1*]
[1*]Department of Chemistry, Institute of Engineering and Technology, Srinivas University, Mukka, Mangaluru, Karnataka 574146, India.
[1]Department of Physics, Bangalore University, Bengaluru, Karnataka-560056, India.
*Corresponding author. E-mail address: susheelakl@bub.ernet.in

Abstract: A new series of barium–lead–praseodymium glass samples was successfully synthesized using the conventional melt-quenching technique. The gamma-radiation shielding performance of the prepared glasses was investigated using the Phy-X/PSD software. The radiation attenuation parameters, including the linear attenuation coefficient (LAC), effective atomic number (Z_{eff}), tenth value layer (TVL), effective conductivity (C_{eff}), and fast neutron removal cross-section (FNRCS), were evaluated over a wide photon energy range of 0.015–15 MeV for five glass compositions containing different concentrations of Pr_2O_3 while maintaining constant BaO content. The results revealed that the LAC values were significantly higher at lower photon energies, indicating superior attenuation behavior in this region. Among all investigated compositions, the glass containing 0% Pr_2O_3 and 10% BaO exhibited the highest LAC and C_{eff} values along with the lowest TVL values, demonstrating excellent radiation shielding capability. The enhanced shielding efficiency was attributed to the presence of high atomic number elements such as barium (Ba, Z = 56) and praseodymium (Pr, Z = 59), which increase the probability of gamma-ray interaction and attenuation. These findings confirm that the incorporation of BaO-rich compositions significantly improves the nuclear radiation shielding effectiveness of the glass system.

Keywords: Effective conductivity , Fast neutron removal cross section, Tenth value layer, Effective Electron density , Linear Attenuation Coefficient.

1. Introduction

In recent decades, have seen the development of new technologies designed to fulfil human requirements. The exposure to radiation in different sectors, including healthcare, is a significant concern that requires attention. Thus, it is important to limit harmful radiation exposure by implementing effective shielding strategies or materials [1-5]. For this purpose, it is important to find suitable materials or devices that can decrease radiation exposure. Choosing the right and effective radiation shielding materials is an important factor that depends on the specific requirements and their application or use. To effectively suppress radiation, it is essential to manufacture radiation shielding components that possess high density, significant stability, excellent radiation attenuation, and are easy to prepare. The primary materials used for radiation shielding are concrete blocks, tiles, and clay bricks. These materials serve as barriers, effectively lowering radiation to safe levels because of their dense structure, affordability, and adaptability [6-8]. Materials such as ceramics [9], glasses [10], polymers [11], and alloys [12] have been studied as effective shielding materials. Among all materials, glasses are considered the most appropriate choice for shielding applications because of their outstanding characteristics, including excellent transparency, stability, high

hardness, compositional resilience, cost-effectiveness, and the simplicity of preparation through various methods [13–15]. Heavy-metal oxide-doped borate glasses exhibit favourable properties for radiation shielding [16-20]. The low melting point of borate enables quick glass preparation with lower risk when utilizing an appropriate furnace. Borate glass possesses essential characteristics, including extensive compositional flexibility, significant optical transparency, high solubility for rare-earth elements, adjustable mechanical durability, outstanding electrical properties, and economical raw materials, prompting researchers to investigate its use across multiple domains [21-25]. Significantly, borate glasses have played an essential role in multiple areas, such as radiation therapy, nuclear medicine, radiation detection, nuclear research, and waste management. Glass containing heavy metal (HM) oxides such as PbO offers exceptional shielding against gamma radiation. Its significant density and the increased effective atomic number of each element in the glass formulation lead to reduced relaxation times and half-layer thicknesses [26]. Various glass systems are designed with multiple components to achieve specific physical, optical, and radiation shielding properties. Among these, barium oxide (BaO) plays a significant role due to its high atomic number and density, which considerably enhance the radiation attenuation capability of glass materials. The incorporation of BaO into borate-based glass systems improves the shielding efficiency against ionizing radiation by increasing the probability of photon interaction within the glass matrix [27-28]. In addition to enhancing radiation protection, BaO also contributes to improved chemical durability and structural stability of the glass network. Furthermore, boron trioxide (B_2O_3), when combined with heavy metal oxides such as barium oxide, provides effective radiation attenuation owing to the increased density and mass attenuation characteristics of the prepared glass system. Therefore, BaO incorporated borate glasses are considered promising materials for advanced radiation shielding applications. Sodium oxide (Na_2O), an alkali metal oxide, is considered an effective glass modifier due to its ability to reduce the melting temperature of glass systems[29].

Rare earth elements are extensively utilized in applications such as polishing, colouring, magnets, lighting systems, and catalytic converters because of their distinctive physical and chemical properties. Light rare earth elements (LREEs), including lanthanum (La), cerium (Ce), praseodymium (Pr), and neodymium (Nd), are relatively more abundant than heavy rare earth elements (HREEs). In contrast, HREEs possess higher atomic numbers and exhibit superior optical, magnetic, and electronic characteristics, making them highly suitable for advanced technological applications such as semiconductors, catalysts, lasers, and photonic devices. Owing to their high atomic numbers, rare earth elements also demonstrate significant radiation shielding and attenuation capabilities in materials such as glass, metal alloys, and polymer matrices [30-31]. The selection of suitable materials for radiation shielding requires a detailed theoretical analysis to accurately evaluate their attenuation performance. Among the available computational tools, Phy-X/PSD software has gained considerable attention for studying the radiation shielding properties of different materials. The software utilizes parameters such as material composition, density, and photon energy to estimate important shielding characteristics, including the mass attenuation coefficient (MAC) and other attenuation parameters. In addition, experimental investigations are essential to validate the

theoretical and computational findings, thereby ensuring the reliability and accuracy of the obtained results.

2. Materials and Methods:

2.1 Experimental Approach:

A collection of glasses was synthesized using the composition (60-x)B_2O_3-(30-y)Na_2O-yBaO - 5PbO-5PbF_2-x Pr_2O_3 (x=0, 0.1, 0.3, 0.5 mol%, y=10%) via the melt-quench method, as detailed in Table 1. The materials used consisted of high-purity of Na_2O, PbO, PbF_2, B_2O_3, Pr_2O_3 and BaO. The concentration of Pr_2O_3 was varied and substituted in place of B_2O_3. All necessary chemicals were quantified, and a 10 g sample of each glass powder was uniformly mixed evenly. The uniform mixed powders were placed into a porcelain crucible and then placed in a muffle furnace for melting at 1000°C for 40 minutes, after which they were quenched onto a brass plate. Thermal annealing was conducted on the quenched glasses at a temperature of 400°C for one hour to relieve the internal stress found in the samples. Finally, we reached room temperature and were polished to the necessary dimensions for further measurements. The measurement of density (ρ) was conducted with toluene as the immersion liquid, determined through Archimedes' principle at room temperature.

Samples	B_2O_3	Na_2O	BaO	PbO	PbF_2	Pr_2O_3	Density (ρ) g/cm^3
Base	60	30	0	5	5	0	3.628
B1	60	20	10	5	5	0	3.759
B2	59.9	20	10	5	5	0.1	3.459
B3	59.7	20	10	5	5	0.3	3.464
B4	59.5	20	10	5	5	0.5	3.422

Table.1 Synthesized glass composition and Density.

2.2 Theoretical analysis was performed employing Phy-X software:

The Phy-X/PSD computational tool serves as an essential resource for assessing the radiation shielding characteristics of glass materials [32].

- The linear attenuation coefficient (LAC) (μ) is one of the most significant parameters used to evaluate the radiation shielding ability of a material. It represents the probability of interaction between incident photons and the shielding medium per unit thickness. The LACs for each synthesized B-Pr glass were determined by calculating the linear slope of the relationship between $\ln \frac{I_0}{I_t}$ and various thicknesses based on (t, cm), using the following expression [33-34].

  $$LAC = \frac{ln\left(\frac{I_0}{I_t}\right)}{t} \quad \ldots\ldots (1)$$

- The TVL value, conversely, represents the thickness of material at which the intensity of incoming radiation is reduced to one-tenth of its original level [34]. Lower TVL values indicate superior

radiation shielding performance because a smaller thickness is sufficient to attenuate gamma radiation [35].

$$TVL = \left(\frac{ln10}{\mu}\right) \quad \ldots\ldots (2)$$

- The effective electron number (N_{eff}) is a key parameter for shielding, indicating the total number of electrons that can engage in photon interactions within the material. A higher N_{eff} value signifies a greater ability to attenuate gamma rays, resulting from an increased chance of photon–electron interactions. The calculated N_{eff} values confirmed the suitability of the prepared glasses for radiation shielding applications over a broad photon energy range [36].We can calculate N_{eff} as follows.

$$N_{eff} = \frac{\mu_m}{\sigma_e} \quad \ldots. (3)$$

- Effective conductivity (C_{eff}), is connected to the electron transport properties of the shielding material and has a strong correlation with the effective electron density. Higher C_{eff} values reflect a boosted probability of interaction between incident radiation and the electrons within the material, thus improving the performance of radiation shielding. C_{eff} of the sample can be calculated by the equation [37].

$$C_{eff} = \left(\frac{N_{eff}\rho e^2 \tau}{m_e}\right) \times 10^3 \quad \ldots\ldots.(4)$$

- The fast neutron removal cross section ($\boldsymbol{\Sigma_R}$) is an essential parameter used to assess the fast neutron shielding capability of a material. It indicates the probability of interaction between fast neutrons and the constituent elements of the shielding medium. Materials exhibiting higher ($\boldsymbol{\Sigma_R}$) values possess superior neutron attenuation efficiency. The fast neutron removal cross section is calculated using[38-39]

$$\left(\Sigma_R = \Sigma\rho_i\left(\Sigma_{\frac{R}{\rho}}\right)\right) \quad \ldots..(5)$$

where (ρ_i) represents the partial density (g/cm³) of the ith constituent and $\boldsymbol{\Sigma_{\frac{R}{\rho}}}$ denotes the mass removal cross section (cm^2/g) of the corresponding element. The obtained ($\boldsymbol{\Sigma_R}$) values provide valuable information regarding the effectiveness of the prepared glass samples for fast neutron shielding applications. Higher ($\boldsymbol{\Sigma_R}$) values indicate enhanced neutron removal capability due to the increased interaction probability between neutrons and the material constituents.

3. Results and Discussion

In this current research, we have examined the nuclear radiation shielding properties of newly developed lead borate glasses that incorporate barium. To estimate the linear attenuation coefficient values, the Phy-X/PSD program was employed across a wide range of photon energies, specifically from 0.015 to 15 MeV.

3.1 Linear Attenuation Coefficient (LAC) :A variation of LAC concerning photon energy. At lower energy levels, the LAC is notably high and sharp, primarily because of the predominance of the photoelectric effect, where photons are entirely absorbed by atomic electrons. The probability of

the photoelectric effect diminishes considerably as photon energy rises. Beyond 0.1 MeV, the ongoing reduction of LAC happens at a more gradual pace due to Compton scattering, which involves photons altering their direction due to energy loss and interactions with the shielding material. Thus, the BaO-$PbPr_2$ glass sample, which demonstrated higher LAC values, would be particularly effective as a radiation shielding material for low-energy radiation sources like X-rays employed in medical imaging [40]. In Figure.1 The three compositions exhibit almost the same LAC trends, as the replacement of Pr_2O_3 from 0 to 0.5 mol% leads to only slight modifications in the overall glass network and elemental composition. While Pr_2O_3 does increase density slightly and has a minimal effect on attenuation, its low concentration does not significantly change the shielding response, which results in the parallel LAC energy-dependent curves that are observed. This explains the similar behaviour of the glasses throughout the energy spectrum, with only minor enhancements-particularly in BaO-PbPr at low photon energies, where small increases in density have a more pronounced effect and it is tabulated in Table.2

Photon Energy	**B1**	**B2**	**B3**	**B4**	**B5**
1.50E-02	95.909	139.119	128.395	129.269	128.401
2.00E-02	72.357	88.343	81.421	81.754	80.989
3.00E-02	25.578	30.782	28.367	28.477	28.204
4.00E-02	12.327	32.901	30.258	30.252	29.843
5.00E-02	7.089	18.594	17.210	17.427	17.407
6.00E-02	4.583	11.640	10.773	10.908	10.895
8.00E-02	2.417	5.643	5.221	5.284	5.274
1.00E-01	4.899	6.157	5.675	5.701	5.649
1.50E-01	1.998	2.390	2.202	2.211	2.189
2.00E-01	1.146	1.318	1.215	1.218	1.206
2.84E-01	0.667	0.732	0.675	0.676	0.669
3.00E-01	0.620	0.676	0.623	0.624	0.617
4.00E-01	0.451	0.477	0.439	0.440	0.435
5.00E-01	0.371	0.386	0.355	0.356	0.351
6.00E-01	0.323	0.333	0.306	0.307	0.303
6.62E-01	0.302	0.310	0.285	0.285	0.282
8.00E-01	0.267	0.272	0.250	0.251	0.248
1.00E+00	0.233	0.236	0.217	0.218	0.215
1.50E+00	0.185	0.187	0.172	0.172	0.170
2.00E+00	0.160	0.163	0.150	0.150	0.148
3.00E+00	0.133	0.139	0.128	0.128	0.126
4.00E+00	0.119	0.127	0.117	0.117	0.116
5.00E+00	0.111	0.121	0.111	0.112	0.110
6.00E+00	0.106	0.117	0.108	0.108	0.107
8.00E+00	0.100	0.115	0.106	0.106	0.105
1.00E+01	0.098	0.115	0.106	0.106	0.105
1.50E+01	0.097	0.119	0.110	0.110	0.109

ISSN: 2096-3246
Volume 58, Issue 01, 2026

Table.2 Calculated values of Linear Attenuation Coefficients (cm^{-1}) using Phy-X/PSD software.

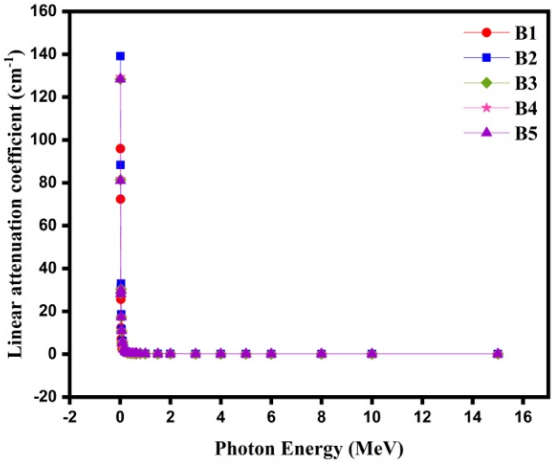

Figure.1 Variation of Linear attenuation coefficient (LAC) with incident photon energy for Synthesized glass samples.

3.2 Tenth Value Layer (TVL): The acquisition of TVL values strengthens the research findings. Looking at Figure.2, the TVL values for photon energy (E= 0.015 to 15 MEV) increase with higher energy levels. A significant shift in TVL values is noted between 0.2 MeV and 8 MeV, with maximum values rising in correlation with the increasing photon energy. The findings confirm that the addition of BaO is the key element in lowering TVL and boosting radiation shielding efficiency. Although Pr_2O_3 doping results in minor improvements at lower energy levels, higher amounts do not lead to further enhancements and might even degrade performance. All the compositions analyzed, B2 (BaO 10%, Pr_2O_3 0%) consistently demonstrates the lowest TVL values, making it the most efficient shielding glass in this group. This emphasizes that altering density with BaO is more significant than rare-earth doping for optimal radiation protection in borate glasses.

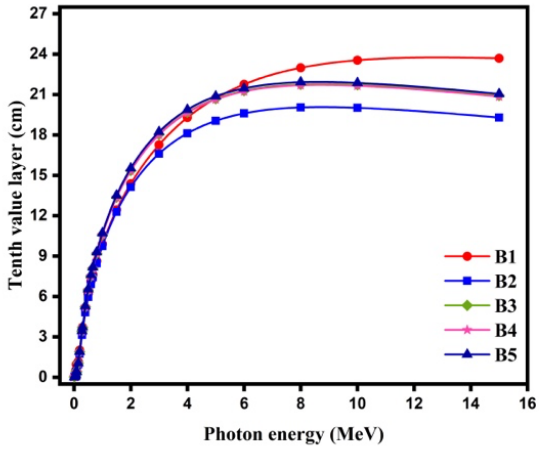

Figure.2 Variation of Tenth Value Layer (TVL) with incident photon energy for Synthesized glass samples

3.3 Effective electron density (N_{eff}): Here values are commonly used to investigate the energy-

ISSN: 2096-3246
Volume 58, Issue 01, 2026

dependent changes in materials designed for alternative radiation shielding. In this analysis, N_{eff} values have been calculated to understand the photon interactions of the glass materials that were used. For Barium borate glasses, the dependencies related to photon energy in the N_{eff} graph have been represented in Figure. 3.The differences in N_{eff} values found for the study area are in agreement with the literature. The results depicted in Fig. 3 indicate that the 10%BaO-Pr 0.5% sample has the minimum N_{eff} value, while the 0% BaO-Pr 0% sample has the maximum N_{eff} value in the lowest energy region, specifically at 0.015MeV.

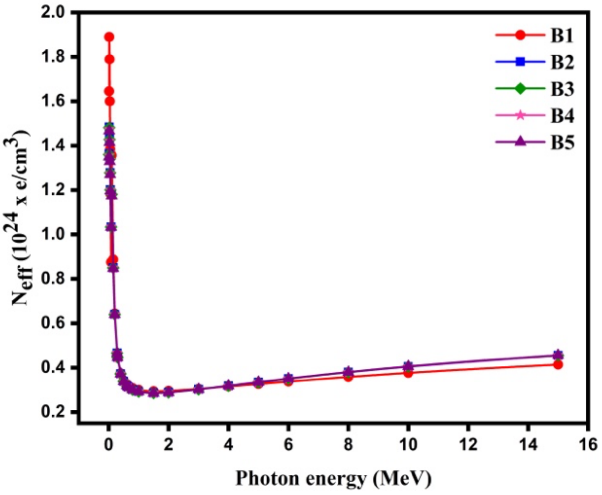

Figure.3 Variation of Effective electron density (N_{eff}) with incident photon energy for Synthesized glass samples

3.4 Effective conductivity (C_{eff}): The effectiveness of our glass samples in shielding was evaluated through the glass effective conductivity (C_{eff}) values. This metric reflects the number of free electrons generated in the material following radiation exposure [41]. Elevated values of this property suggest a greater absorption of radiation. Higher values of this characteristic suggest an increased absorption of radiation. Figure 4 demonstrates the variation of C_{eff} values in relation to the energy of incident photons. The C_{eff} values fluctuate based on the energy of the photons and the content of CeO_2, as depicted in the figure. At lower photon energies, the photoelectric effect prevails, leading to higher C_{eff} values. The glass containing Pr_2O_3 (0 mol%) evidently exhibits superior radiation shielding capabilities. Additionally, at elevated energy levels, both Pr_2O_3-0% and BaO-10% show enhanced radiation shielding effectiveness.

ISSN: 2096-3246
Volume 58, Issue 01, 2026

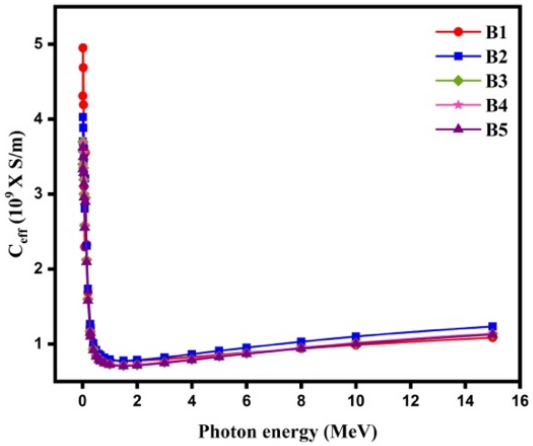

Figure.4 Variation of Effective conductivity (C_{eff})with incident photon energy for Synthesized glass samples

3.5 (FNRCS):Fast neutron removal cross section (ΣR): Additionally, the ∑R values were determined for the BaO-PbPr borate glass system. The methods for calculating ∑R for all glass types are outlined in Table 3. The ∑R results ranged from 0.128 cm^{-1} to 0.101 cm^{-1}. Table 3 presents a comparison of the fast neutron removal cross sections of the glasses examined with several commonly utilized neutron shielding materials. It is observed that the ∑R values of the current glasses exceed those of graphite and hematite-serpentine concrete, being very similar to those of water and $Bi_4O_3B_2O$ glass.

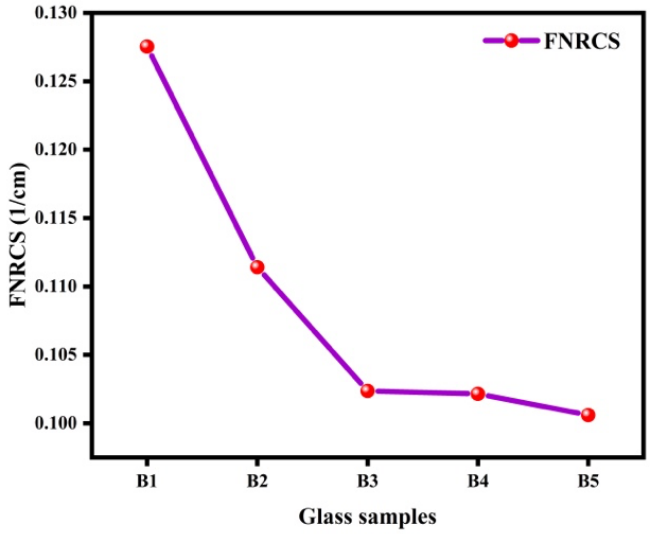

Figure.5 Variation of Fast neutron removal cross section (ΣR) with Synthesized glass samples

Samples	∑R (cm^{-1})
SBC-B00	0.0927
SBC-B10	0.0946
SBC-B20	0.0962
SBC-B30	0.0965
SBC-B35	0.0971
$Bi_4O_3B_2O$	0.1034
Water (H_2O)	0.1023
Graphite (C)	0.0772
Hematite-serpentine concrete	0.0975
B1	0.128
B2	0.111
B3	0.102
B4	0.102
B5	0.101

Table. 3 Comparison Fast neutron removal cross section (ΣR) with Synthesized glasses and other materials

4. Conclusion

The current work highlights five barium-PbPr borate glasses that have been identified for their role in radiation protection applications. As the level of Pr_2O_3 increased from 0.0 to 0.5 mol%, the density (ρ) of the glass gradually fell from 3.6286 to 3.4220 $g.cm^{-3}$. It has been determined that BaO at a concentration of 10 mol% significantly contributes to the protective effectiveness of the proposed glasses against gamma rays and fast neutrons. When it comes to radiation shielding, choosing the right glass should be guided by data on LAC, N_{eff}, TVL, C_{eff}, as well as the evaluation of neutron removal cross sections, tailored to the specific application in mind. At a concentration of BaO-10 mol% and Pr_2O_3-0%, the LAC and N_{eff} values rise while the TVL and C_{eff} values decline. Therefore, the BaO-PbPr-0% glass stands out as a superior option for shielding against gamma rays and fast neutrons compared to various conventional concrete and commercial glasses.

Acknowledgement

The author (SKL) acknowledges financial support from the Vision Group on Science and Technology (VGST), Government of Karnataka, under KSTEPS/VGST/ECRA/GRD No. 1251/2023-24

References

1. Chaiphaksa, W., Borisut, P., Chanthima, N., Kaewkhao, J., & Sanwaranatee, N. W. (2022). Mathematical calculation of gamma rays interaction in bismuth gadolinium silicate glass using WinXCom program. *Materials Today: Proceedings, 65*, 2412–2415.

2. Dong, M. (2025). From mineral to high-value shielding material: Conversion of ludwigite into polyimide resin-based composites for medical X-rays protection. *Nexus Future Materials, 2*, 610992.
3. Lakshminarayana, G., Dong, M. G., Al-Buriahi, M. S., Kumar, A., Lee, D.-E., Yoon, J., & Park, T. (2020). B_2O_3–Bi_2O_3–TeO_2–BaO and TeO_2–Bi_2O_3–BaO glass systems: A comparative assessment of gamma-ray and fast and thermal neutron attenuation aspects. *Applied Physics A, 126*, 202.
4. Manjunatha, M. M., Hosamani, G. B., Hiremath, A., Vinayak, V. P., Singh, A. S., & Bennal, N. M. (2023). An experimental approach to determine the gamma radiation interaction mean free path and exposure buildup factor for biomolecules. *Applied Radiation and Isotopes, 201*, 111012.
5. Mhareb, M. H. A., Mekki, A., Alwabsi, A., Almaimouni, A., Thabit, H. A., Alshwaira, N., Alsaleh, I. A., & Al-Dhahi, F. A. (2024). X-ray photoelectron spectroscopy, structural, and radiation shielding properties for transparent borosilicate glasses. *Optical Materials, 152*, 115488.
6. Krishnaih, K. V., Venkatramu, V., & Jayasankar, C. K. (2018). Lanthanide-doped tellurite glasses for solar energy harvesting. In R. El-Mallawany (Ed.), *Tellurite Glass Smart Materials – Applications in Optics and Beyond* (pp. 249–274). Springer. https://doi.org/10.1007/978-3-319-76568-6_11
7. Kumar, K. U., Babu, P., Basavapoornima, C., Praveena, R., Rani, D. S., & Jayasankar, C. K. (2022). Spectroscopic properties of Nd^{3+}-doped boro-bismuth glasses for laser applications. *Physica B: Condensed Matter, 646*, 414327. https://doi.org/10.1016/j.physb.2022.414327
8. Lakshminarayana, G., Baki, S. O., Sayyed, M. I., Dong, M. G., Lira, A., Noora, A. S. M., Kityk, I. V., & Mahdia, M. A. (2018). Vibrational, thermal features, and photon attenuation coefficients evaluation for TeO_2–B_2O_3–BaO–ZnO–Na_2O–Er_2O_3–Pr_6O_{11} glasses as gamma-rays shielding materials. *Journal of Non-Crystalline Solids, 481*, 568–578. https://doi.org/10.1016/j.jnoncrysol.2017.11.049
9. Modifier's influence on spectral properties of dysprosium ions doped lead boro-telluro-phosphate glasses for white light applications. (2022). *Optics & Laser Technology, 156*, 108585. https://doi.org/10.1016/j.optlastec.2022.108585
10. Al-Buriahi, M. S., Eke, C., Alomairy, S., Yildirim, A., Alsaeedy, H. I., & Sriwunkum, C. (2021). Radiation attenuation properties of some commercial polymers for advanced shielding applications at low energies. *Polymer Advanced Technologies, 32*, 2386–2396. https://doi.org/10.1002/pat.5267
11. Kaur, T., Sharma, J., & Singh, T. (2017). Feasibility of Pb-Zn binary alloys as gamma shielding materials. *International Journal of Pure and Applied Physics, 13*, 222–225.
12. Almuqrin, A. H., & Sayyed, M. I. (2021). Radiation shielding characterizations and investigation of TeO_2–WO_3–Bi_2O_3 and TeO_2–WO_3–PbO glasses. *Applied Physics A, 127*, 190. https://doi.org/10.1007/s00339-021-04344-9

13. Chandrappa, V., Basavapoornima, C., Kesavulu, C. R., Babu, A. M., Depuru, S. R., & Jayasankar, C. K. (2022). Spectral studies of Dy^{3+}: zinc phosphate glasses for white light source emission applications: A comparative study. *Journal of Non-Crystalline Solids, 583*, 121466. https://doi.org/10.1016/j.jnoncrysol.2022.121466
14. Ramprasad, P., Basavapoornima, C., Depuru, S. R., & Jayasankar, C. K. (2022). Spectral investigations of Nd^{3+}:$Ba(PO_3)_2$+La_2O_3 glasses for infrared laser gain media applications. *Optical Materials, 129*, 112482. https://doi.org/10.1016/j.optmat.2022.112482
15. Sathiyapriya, G., Divina, R., Marimuthu, K., Vijayakumar, M., Lacomme, E., & Sayyed, M. I. (2021). Exploration on dysprosium ions doped zinc barium boro-tellurite glasses towards radiation screening and photonic applications. *Physica B: Condensed Matter, 612*, 412991. https://doi.org/10.1016/j.physb.2021.412991
16. Abouhaswa, A. S., & Kavaz, E. (2020a). Bi_2O_3 effect on physical, optical, structural and radiation safety characteristics of B_2O_3–Na_2O–ZnO–CaO glass system. *Journal of Non-Crystalline Solids, 535*, 119993.
17. Abouhaswa, A. S., & Kavaz, E. (2020b). A novel B_2O_3–Na_2O–BaO–HgO glass system: Synthesis, physical, optical and nuclear shielding features. *Ceramics International, 46*, 16166–16177.
18. Katubi, K. M., Basha, B., Alsufyani, S. J., Alrowaili, Z. A., Sriwunkum, C., Alnairi, M. M., & Al-Buriahi, M. S. (2023). Radiation attenuation and optical properties of P_2O_5-based glass system. *Journal of Radiation Research and Applied Sciences, 16*, 100688. https://doi.org/10.1016/j.jrras.2023.100688
19. Rajesh, M., & Kavaz, E. (2021). Photoluminescence and radiative shielding properties of Sm^{3+} ions doped fluoroborosilicate glasses for visible reddish-orange display and radiation shielding applications. *Materials Research Bulletin, 142*, 111383.
20. Sayyed, M. I., Mahmoud, K. A., Biradar, S., Rilwan, U., & Najam, L. A. (2025). Dual-purpose borate based glasses: Optical features and Monte Carlo simulations of gamma radiation shielding. *Nuclear Engineering and Technology, 57*, 103752.
21. Almuqrin, A. H., Rashad, M., More, C. V., Sayyed, M. I., & Elsafi, M. (2024). An experimental and theoretical study to evaluate Al_2O_3–PbO–B_2O_3–SiO_2–BaO radiation shielding properties. *Radiation Physics and Chemistry, 222*, 111824.
22. Alzahrani, F. M. A., Albarkaty, K. S., Çalışkan, F., Olarinoye, I. O., & Al-Buriahi, M. S. (2023). Physical, microstructural, and radiation energy absorption properties of recycled CRT-screen glass doped with Bi_2O_3. *Journal of Radiation Research and Applied Sciences, 16*, 100727. https://doi.org/10.1016/j.jrras.2023.100727
23. Kaky, K. M., Altimari, U., & Kadhim, A. J. (2025). Analytical and comparative study on the impact of CaO on the γ-ray shielding performance of borate-based glasses. *Nexus Future Materials, 2*, 172–176.
24. Sayyed, M. I., Biradar, S., More, C. V., & Issa, S. A. M. (2025). Compositional tuning of ZnO/RE-doped borate glasses for enhanced optical and gamma shielding properties. *Radiation Physics and Chemistry*, 113245.

25. Sayyed, M. I., Hamad, D., & Rashad, M. (2024). The role of ZnO in the radiation shielding performance of newly developed B_2O_3–PbO–ZnO–CaO glass systems. *Radiation Physics and Chemistry, 223*, 111896.
26. Zhang, X., Chen, Q., & Zhang, S. (2021). Ta_2O_5 nanocrystals strengthened mechanical, magnetic, and radiation shielding properties of heavy metal oxide glass. *Molecules, 26*(15), 4494. https://doi.org/10.3390/molecules26154494
27. Sayyed, M. I., Bilal, S., Mee, C. V., & Mahmoud, K. A. (2025). Investigation of the optical and gamma-ray attenuation performance of borate-based glasses: Influence of BaO, ZnO, and CaO doping. *Annals of Nuclear Energy, 221*, 111857.
28. Saddeek, B. (2021). Alteration of optical, structural, mechanical durability and nuclear radiation attenuation properties of barium borosilicate glasses through BaO reinforcement: Experimental and numerical analyses. *Ceramics International, 47*, 5587–5596.
29. Alan, H. Y. (2025). Radiation shielding performance of sodium silicate glasses with oxide additives. *Journal of the Korean Physical Society, 88*(4), 429–442. https://doi.org/10.1007/s40042-025-01523-2
30. Kozlovskiy, A. L., & Zdorovets, M. V. (2021). Effect of doping of $Ce^{4+/3+}$ on optical, strength and shielding properties of $(0.5-x)TeO_2$–$0.25MoO_3$–$0.25Bi_2O_3$–$xCeO_2$ glasses. *Materials Chemistry and Physics, 263*, 124444.
31. Solak, B. B., Atlas, R., Inalç, D., Kilic, S., Yalcin, S., Kilicoglu, A., & Demircan, G. (2024). Exploring the radiation shielding properties of B_2O_3–PbO–TeO_2–CeO_2–WO_3 glasses: A comprehensive study on structural, mechanical, gamma attenuationandattenuation characteristics. *Materials Physics and Mechanics, 52*, 126672.
32. Hordieiev, Y. S., & Zaichuk, A. V. (2025c). Lanthanum-doped zinc borate glasses: fabrication, structural analysis, thermal properties, and gamma radiation shielding performance. Journal of Ovonic Research, 21(1), 85–94. https://doi.org/10.15251/jor.2025.211.85
33. Abdelghany, A. M., & Rammah, Y. S. (2021). Transparent alumino lithium borate glass-ceramics: Synthesis, structure and gamma-ray shielding attitude. *Journal of Inorganic and Organometallic Polymers and Materials, 31*, 2560–2568.
34. Alfryyan, N., Alsaif, N. A. M., Al-Ghamdi, H., Abouhaswa, A. S., Sadeq, M. S., Abdelghany, A. M., Kotb, S. M., Talaat, S., & Rammah, Y. S. (2024). Role of ZnO reinforced B_2O_3–BaF_2–Pr_6O_{11}–Na_2O glasses: Synthesis, physical, linear optical properties and γ-ray attenuation efficacy. *Optical and Quantum Electronics, 57*, 56.
35. Alzuhair, A. Z., Alqahtani, M. S., Alkulib, A. J., Hussein, K. I., Reben, M., & Yousef, E. (2022). Structural and shielding properties of the tellurite–tungsten glass matrix with addition zinc fluoride. *Chalcogenide Letters, 19*(3), 187–195. https://doi.org/10.15251/CL.2022.193.187
36. Han, I., & Demir, L. (2009). Studies on effective atomic numbers and electron densities from mass attenuation coefficients in Ti_xCo_{1-x} and Co_xCu_{1-x} alloys. *Nuclear Instruments and Methods in Physics Research Section B: Beam Interactions with Materials and Atoms, 267*, 3505–3510. https://doi.org/10.1016/j.nimb.2009.08.022

37. Tekin, H. O., Bilal, G., Zakaly, H. M. H., Kilic, G., Issa, S. A. M., Ahmed, E. M., Rammah, Y. S., & Ene, A. (2021). Newly developed vanadium-based glasses and their potential for nuclear radiation shielding aims: A Monte Carlo study on gamma ray attenuation parameters. *Materials, 14*(14), 3897. https://doi.org/10.3390/ma14143897
38. Kaur, P., Singh, K., Kurudirek, M., & Thakur, S. (2019). *Spectrochimica Acta Part A: Molecular and Biomolecular Spectroscopy, 223*, 117309.
39. Tekin, H., Kilicoglu, O., Kavaz, E., Altunsoy, E., Almatari, M., Agar, O., & Sayyed, M. (2019). *Results in Physics, 12*, 1797.
40. Echeweozo, E., Katubi, K. M., Alsaiari, N. S., & Al-Buriahi. (2025). A Computational Study of Zr 2 Co Alloy Doped with Pb, Tl, Sn, In, Ga, and Al Elements for Radiation-Shielding Applications. *Nuclear Technology*, 1–10. https://doi.org/10.1080/00295450.2025.2525716
41. Alrowaili, Z. A., Taha, T. A., Ibrahim, M., & Saron, K. M. A. (2021). Investigation of the structure and radiation shielding properties of borate/Y2O3 glasses. *The European Physical Journal Plus*, *136*(5). https://doi.org/10.1140/epjp/s13360-021-01565-y